Full Paper

Applied Organometallic Chemistry

Received: 9 August 2009 Revised: 3 October 2009 Accepted: 5 October 2009 Published online in Wiley Interscience: 30 November 2009

(www.interscience.com) DOI 10.1002/aoc.1581

Novel drug-based Fe(III) heterochelates: synthetic, spectroscopic, thermal and *in-vitro* antibacterial significance

D.H. Jani[a], H.S. Patel[a], H. Keharia[b] and C.K. Modi[c]*

A series of novel heterochelates of the type $[Fe(A^n)(L)(H_2O)_2]\bullet mH_2O$ [where H_2A^n = 4,4′-(arylmethylene)bis(3-methyl-1-phenyl-4,5-dihydro-1H-pyrazol-5-ol); aryl = 4-nitrophenyl, $m = 1$ (H_2A^1); 4-chlorophenyl, $m = 2$ (H_2A^2); phenyl, $m = 2$ (H_2A^3); 4-hydroxyphenyl, $m = 2$ (H_2A^4); 4-methoxyphenyl, $m = 2$ (H_2A^5); 4-hydroxy-3-methoxyphenyl, $m = 1.5$ (H_2A^6); 2-nitrophenyl, $m = 1.5$ (H_2A^7); 3-nitrophenyl, $m = 0.5$ (H_2A^8); *p*-tolyl, $m = 1$ (H_2A^9) and HL = 1-cyclopropyl-6-fluoro-4-oxo-7-(piperazin-1-yl)-1,4-dihydroquinoline-3-carboxylic acid] were investigated. They were characterized by elemental analysis (FT-IR, ^{1}H- & ^{13}C-NMR, and electronic) spectra, magnetic measurements and thermal studies. The FAB-mass spectrum of $[Fe(A^3)(L)(H_2O)_2]\bullet 2H_2O$ was determined. Magnetic moment and reflectance spectral studies revealed that an octahedral geometry could be assigned to all the prepared heterochelates. Ligands (H_2A^n) and their heterochelates were screened for their *in-vitro* antibacterial activity against *Bacillus subtilis, Staphylococcus aureus, Escherichia coli* and *Serratia marcescens* bacterial strains. The kinetic parameters such as order of reaction (*n*), the energy of activation (E_a), the pre-exponential factor (*A*), the activation entropy ($\Delta S^{\#}$), the activation enthalpy ($\Delta H^{\#}$) and the free energy of activation ($\Delta G^{\#}$) are reported.

Keywords: Fe(III) heterochelates; bis-pyrazolones; spectroscopic; thermal studies; *in-vitro* antibacterial activity

Introduction

Iron plays a crucial role in the survival of terrestrial organisms and participates in biochemical processes like ribonucleic reduction, energy production, photosynthesis, nitrogen reduction, oxygen transport and oxygenation.[1] Fluoroquinolone drugs are known for their wide range of applications in medicinal and life sciences.[2] They are typically polyfunctional compounds, designed to interact with specific receptors or organs. The design of metal–fluoroquinolone drug complexes is of particular interest in pharmacological research to improve the drugs activity and to decrease their toxicity. Transition metal complexes of these antibiotics with enhanced potentiality against bacterial strains have been reported elsewhere.[3–6] Ciprofloxacin [1-cyclopropyl-6-fluoro-1, 4-dihydro-4oxo-7-(1-piperazinyl)-3quinolone carboxylic acid] is a synthetic fluoroquinolone antibiotic with a broad spectrum of activity. It is active against a wide variety of aerobic Gram-negative and Gram-positive bacteria. Turel[7] prepared copper(II) ciprofloxacin complexes and tested them against the growth of various Gram-positive and Gram-negative microorganism. These complexes showed comparable antimicrobial activity with the free ligand.

Pyrazolone-5 derivatives form an important class of organic compounds and represent a major scientific and applied interest in biological, analytical applications, catalysis, dye and extraction metallurgy.[8–12] Furthermore, they have the potential to form different types of coordination compounds due to the several electron-rich donor centers.[13,14] Meanwhile, the design of new bis-pyrazolone-based chelating ligands in coordination chemistry has been extensively investigated.[15–24] The studies on bis-pyrazolone-based complexes reveal that they have strong fluorescence properties[25–27] and some of them have antitumor activities *in vitro* and high herbicidal activities.

Accordingly, we have synthesized a series of bis-pyrazolone based ligands, 4,4′-(arylmethylene)bis(3-methyl-1-phenyl-4,5-dihydro-1H-pyrazol-5-ol) (H_2A^n). This new type of chelating ligand has two donor cites centered at 5,5′-OH groups. Because of the presence of two active donor sites, they can form various types of metal complexes. In continuation to our earlier work on bis-pyrazolone based compounds,[28–30] herein we describe synthetic, spectroscopic, thermal and *in-vitro* antibacterial studies of some novel drug-based Fe(III) heterochelates. The general structure of the ligands (H_2A^n) is shown in Scheme 1.

Materials and Methods

Materials

All the chemicals used were of analytical grade and used without further purification. The compound 1-phenyl-3-methyl-2-pyrazoline-5-ol was purchased from E. Merck Ltd (India).

* *Correspondence to: C.K. Modi, Department of Chemistry, Bhavnagar University, Bhavnagar-364 002, Gujarat, India. E-mail: modi_ck@yahoo.co.in*

a *Department of Chemistry, Sardar Patel University, Vallabh Vidyanagar-388 120, Gujarat, India*

b *Department of Bio Sciences, Sardar Patel University, Vallabh Vidyanagar-388 120, Gujarat, India*

c *Department of Chemistry, Bhavnagar University, Bhavnagar-364 002, Gujarat, India*

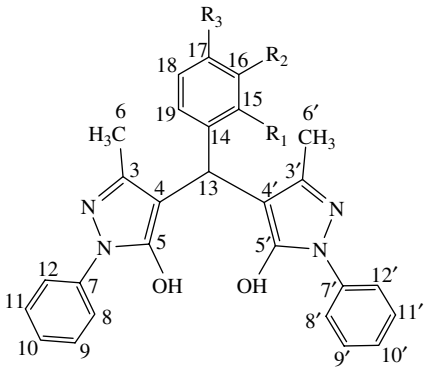

Ligands	R_1	R_2	R_3
H_2A^1	-H	-H	$-NO_2$
H_2A^2	-H	-H	-Cl
H_2A^3	-H	-H	-H
H_2A^4	-H	-H	-OH
H_2A^5	-H	-H	$-OCH_3$
H_2A^6	-H	$-OCH_3$	-OH
H_2A^7	-H	$-NO_2$	-H
H_2A^8	$-NO_2$	-H	-H
H_2A^9	-H	-H	CH_3

Scheme 1. The general structure of ligands (H_2A^n).

4-Substituted benzaldehydes were purchased from Qualigens Fine Chemicals, India and used without further purification. Ciprofloxacin hydrochloride was purchased from Bayer AG (Wuppertal, Germany). The organic solvents were purified by standard methods.[31] Luria broth was purchased from Hi-media Laboratories Pvt. Ltd, India.

Instruments

Carbon, hydrogen and nitrogen were analyzed with a Perkin Elmer, USA 2400-II CHN analyzer. The metal contents of the heterochelates were analyzed by EDTA titration[32] after decomposing the organic matter with a mixture of concentrated $HClO_4$, H_2SO_4 and HNO_3 (1 : 1.5 : 2.5). Infrared spectra (4000–400 cm^{-1}) were recorded on Nicolet-400D spectrophotometer using KBr pellets. ^{1}H- and ^{13}C-NMR and DEPT-135 spectra were recorded on a model Advance 400 Bruker FT-NMR instrument and DMSO-d_6 used as a solvent. The FAB mass spectrum of the heterochelate was recorded at SAIF, CDRI, Lucknow with Jeol SX-102/DA-6000 mass spectrometer. The magnetic moments were obtained by the Gouy's method using mercury tetrathiocyanato cobaltate (II) as a calibrant ($g = 16.44 \times 10^{-6}$ c.g.s. units at 20 °C). Diamagnetic corrections were made using Pascal's constant. The reflectance spectra of the free ligands (H_2A^n) and their heterochelates were recorded in the range 1700–350 nm (as MgO disks) on a Beckman DK-2A spectrophotometer. A simultaneous •TG/DTG was obtained by a model 5000/2960 SDT, TA Instruments, USA. The experiments were performed in an N_2 atmosphere at a heating rate of 10 °C min^{-1} in the temperature range 50–800 °C, using an Al_2O_3 crucible. The sample sizes ranged in mass from 5 to 8 mg. The DSC was recorded using a DSC 2920, TA Instruments, USA. The DSC curves were obtained at a heating rate of 10 °C min^{-1} in an N_2 atmosphere over the temperature range 50–400 °C, using an aluminum crucible.

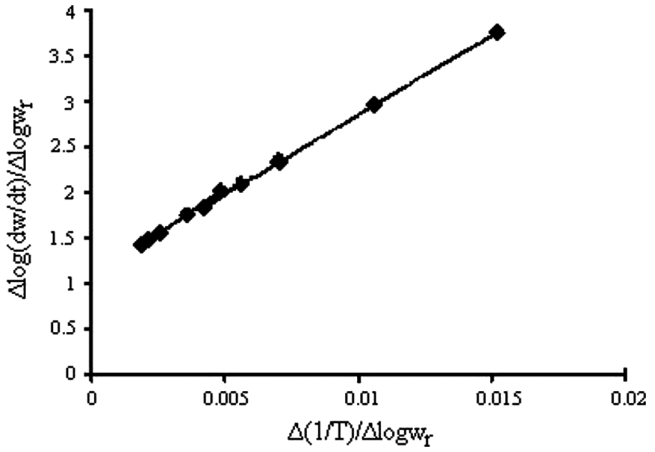

Figure 2. Freeman–Carroll plot of the heterochelate [Fe(A^5)(L)$(H_2O)_2$]•$2H_2O$.

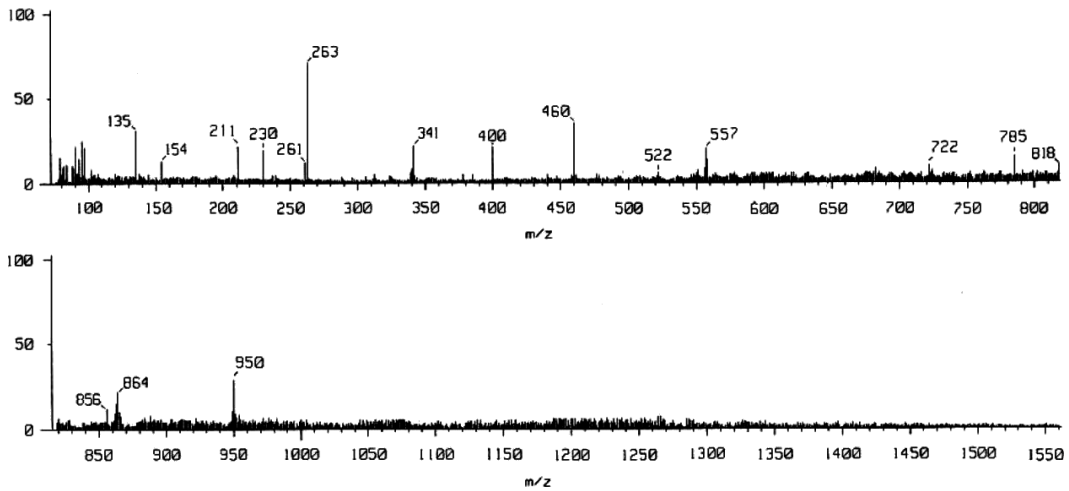

Figure 1. FAB mass spectra of the heterochelate [Fe(A^3)(L)$(H_2O)_2$]•$2H_2O$.

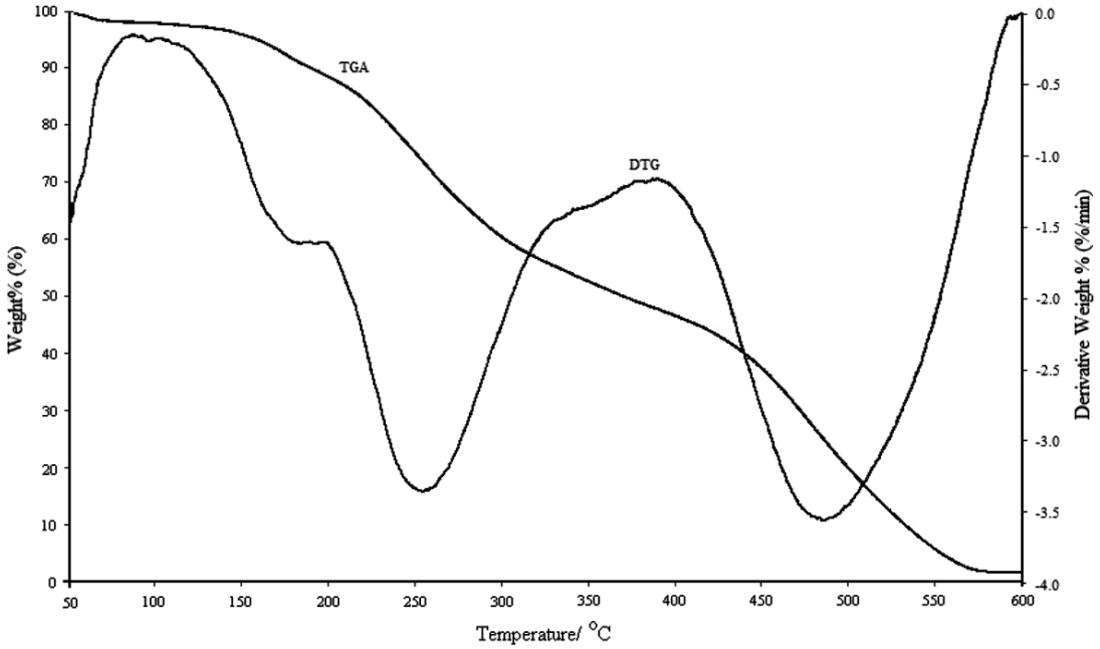

Figure 3. TGA/DTG curves of the heterochelate $[Fe(A^5)(L)(H_2O)_2]^{\bullet}2H_2O$.

Synthesis of Ligands (H_2A^1–H_2A^9)

The dinegative bidentate ligands were synthesized by condensation of 3-methyl-1-phenyl-2-pyrazoline-5-one (10 mmol), with various substituted benzaldehydes (5 mmol), in the presence of catalytic amounts of sodium dodecyl sulfate (SDS).

4,4′-[(4-Nitrophenyl)methylene]bis(3-methyl-1-phenyl-4,5-dihydro-1H-pyrazol-5-ol) (H_2A^1)

An ethanolic solution (50 ml) of 3-methyl-1-phenyl-2-pyrazoline-5-one (10 mmol, 2.16 g) and an ethanolic solution (25 ml) of 4-nitrobenzaldehyde (5 mmol, 0.76 g) in 2 : 1 molar ratio with a catalytic amount of SDS in aqueous solution (5 ml) were mixed together at room temperature with constant stirring for 30 min and then refluxed for 3 h on a water bath. The resulting mixture was then allowed to stand overnight at room temperature. The pinkish products formed were collected by filtration, washed with diethyl ether and dried *in vacuo* to constant mass and then finally purified by crystallized in chloroform–hexane (70 : 30) mixture to obtain pink crystalline products. Yield, 86%; m.p. 228–230 °C. Found (%): C, 67.60, H, 4.74, N, 14.44. $C_{27}H_{23}N_5O_4$ (481.50) requires (%): C, 67.35, H, 4.81, N, 14.54. IR: 3392 (O–H), 1600 (C═O); ^{1}H-NMR: 2.30

Table 1. Physical and analytical data of the heterochelates

Sample no.	Compounds	Formula weight (g mol^{-1})	Color (yield%)	Melting point (°C)	Analysis (%) Found (calcd) C	H	N	M	μ_{eff} (B.M.)
1	$[Fe(A^1)(L)(H_2O)_2]^{\bullet}H_2O$ $C_{44}H_{48}FFeN_8O_{10}$	923.73	Reddish brown (79)	214	57.20 (57.21)	5.25 (5.24)	12.12 (12.13)	6.03 (6.05)	5.98
2	$[Fe(A^2)(L)(H_2O)_2]^{\bullet}2H_2O$ $C_{44}H_{50}ClFFeN_7O_9$	931.18	Reddish brown (83)	188	56.72 (56.75)	5.40 (5.41)	10.52 (10.53)	6.00 (6.00)	6.05
3	$[Fe(A^3)(L)(H_2O)_2]^{\bullet}2H_2O$ $C_{44}H_{51}FFeN_7O_9$	896.73	Reddish brown (85)	204	58.90 (58.93)	5.71 (5.73)	10.95 (10.93)	6.21 (6.23)	5.95
4	$[Fe(A^4)(L)(H_2O)_2]^{\bullet}2H_2O$ $C_{44}H_{51}FFeN_7O_{10}$	912.73	Orange (88)	176	57.88 (57.90)	5.63 (5.63)	10.73 (10.74)	6.10 (6.12)	5.99
5	$[Fe(A^5)(L)(H_2O)_2]^{\bullet}2H_2O$, $C_{45}H_{53}FFeN_7O_{10}$	926.76	Dark green (86)	195	58.30 (58.32)	5.72 (5.76)	10.55 (10.58)	6.01 (6.03)	6.01
6	$[Fe(A^6)(L)(H_2O)_2]^{\bullet}1.5H_2O$ $C_{45}H_{52}FFeN_7O_{10.5}$	933.76	Dull orange (90)	289	57.85 (57.88)	5.60 (5.61)	10.48 (10.50)	5.96 (5.98)	6.07
7	$[Fe(A^7)(L)(H_2O)_2]^{\bullet}1.5H_2O$ $C_{44}H_{49}FFeN_8O_{10.5}$	932.73	Reddish brown (85)	273	56.65 (56.66)	5.27 (5.29)	12.00 (12.01)	5.98 (5.99)	6.15
8	$[Fe(A^8)(L)(H_2O)_2]^{\bullet}0.5H_2O$ $C_{44}H_{47}FFeN_8O_{9.5}$	914.73	Reddish brown (81)	294	57.76 (57.77)	5.15 (5.18)	12.22 (12.25)	6.10 (6.11)	5.98
9	$[Fe(A^9)(L)(H_2O)_2]^{\bullet}H_2O$ $C_{45}H_{51}FFeN_7O_8$	892.76	Orange (92)	297	60.53 (60.54)	5.75 (5.76)	10.97 (10.98)	6.25 (6.26)	5.97

Table 2. The characteristic IR bands of ligand (HL)[a] and their heterochelates

Compounds	$\nu_{(O-H)}$	$\nu_{(O-H)}$[b]	$\nu_{(C=O)}$	$\nu_{(COO-)}$ Antisymmetric	$\nu_{(COO-)}$ Symmetric	$\Delta\nu$	$\nu_{(C-O)}$	$\nu_{(M-O)}$	$\nu_{(M-O)}$[c]
HL	–	1707	1635	1618	1384	234	–	–	–
$[Fe(A^1)(L)(H_2O)_2]^{\bullet}H_2O$	3418	–	1624	1600	1384	216	1316	449	420
$[Fe(A^2)(L)(H_2O)_2]^{\bullet}2H_2O$	3422	–	1620	1600	1384	216	1305	472	418
$[Fe(A^3)(L)(H_2O)_2]^{\bullet}2H_2O$	3430	–	1624	1598	1384	214	1309	448	419
$[Fe(A^4)(L)(H_2O)_2]^{\bullet}2H_2O$	3438	–	1625	1600	1380	220	1303	449	420
$[Fe(A^5)(L)(H_2O)_2]^{\bullet}2H_2O$	3435	–	1626	1597	1380	217	1312	448	417
$[Fe(A^6)(L)(H_2O)_2]^{\bullet}1.5H_2O$	3330	–	1624	1597	1384	213	1308	449	417
$[Fe(A^7)(L)(H_2O)_2]^{\bullet}1.5H_2O$	3420	–	1620	1599	1380	219	1303	449	418
$[Fe(A^8)(L)(H_2O)_2]^{\bullet}0.5H_2O$	3428	–	1620	1599	1384	215	1306	448	415
$[Fe(A^9)(L)(H_2O)_2]^{\bullet}H_2O$	3430	–	1622	1600	1384	216	1310	444	428

[a] HL = 1-cyclopropyl-6-fluoro-4-oxo-7-(piperazin-1-yl)-1,4-dihydroquinoline-3-carboxylic acid. [b] $\nu_{(O-H)}$ of the carboxylic group; [c] $\nu_{(M-O)}$ of the ketone group of HL.

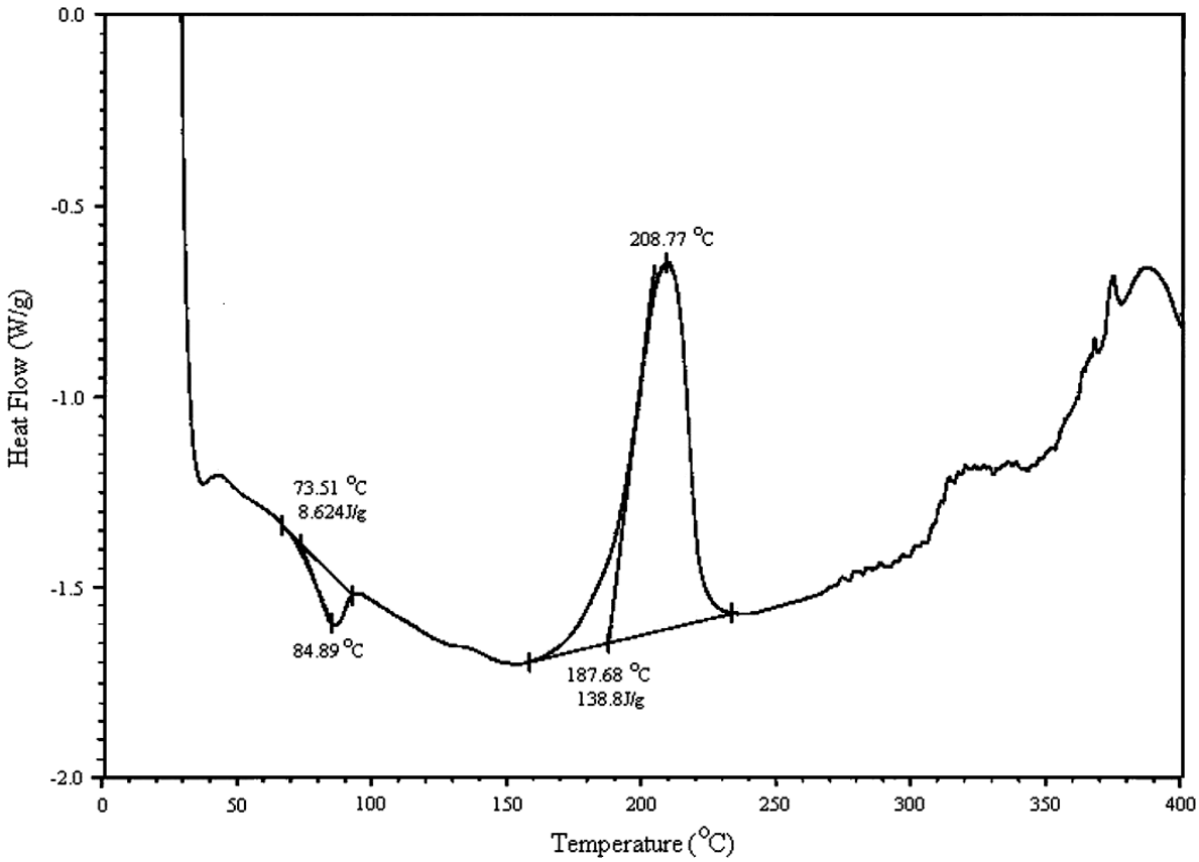

Figure 4. DSC curve of the heterochelate $[Fe(A^5)(L)(H_2O)_2]^{\bullet}2H_2O$.

(6H, s, protons at C_6, $C_{6'}$), 5.10 (1H, s, protons at C_{13}), 7.20–8.10 (14H, m, protons at C_8–H, C_9–H, C_{10}–H, C_{11}–H, C_{12}–H, C_{15}–H, C_{16}–H, C_{18}–H, C_{19}–H, $C_{8'}$–H, $C_{9'}$–H, $C_{10'}$–H, $C_{11'}$–H, $C_{12'}$–H), 12.60 (1H, s, protons -OH), 13.80 (1H, s, protons H···OH); ^{13}C-NMR: 11.40 (C_6, $C_{6'}$), 33.60 (C_{13}), 121.50 (C_4, $C_{4'}$), 123.60 (C_8, C_{12}, $C_{8'}$, $C_{12'}$), 126.70 (C_{10}, $C_{10'}$), 128.10 (C_{16}, C_{18}), 129.02 (C_9, C_{11}, C_{15}, C_{19}, $C_{9'}$, $C_{11'}$), 136.34 (C_7, $C_{7'}$), 146.12 (C_{14}), 146.55 (C_{17}), 148.30 (C_3, $C_{3'}$), 157.76 (C_5, $C_{5'}$); DEPT-135: 11.30 (C_6, $C_{6'}$), 33.60 (C_{13}), 121.50 (C_4, $C_{4'}$), 123.60 (C_8, C_{12}, $C_{8'}$, $C_{12'}$), 126.70 (C_{10}, $C_{10'}$), 128.10 (C_{16}, C_{18}), 129.04 (C_9, C_{11}, C_{15}, C_{19}, $C_{9'}$, $C_{11'}$).

4,4′-[(4-Chlorophenyl)methylene]bis(3-methyl-1-phenyl-4,5-dihydro-1H-pyrazol-5-ol) (H_2A^2)

H_2A^2 was synthesized by same method used for H_2A^1 using 4-chlorobenzaldehyde instead of 4-nitrobenzaldehyde. Yield, 88%; m.p. 207–209 °C. Found (%): C, 68.92, H, 4.93, N, 11.83. $C_{27}H_{23}N_4O_2Cl$ (470.93) requires (%): C, 68.86, H, 4.81, N, 11.89. IR: 3400 (O–H), 1600 (C=O); ^{1}H-NMR: 2.36 (6H, s, protons at C_6, $C_{6'}$), 4.90 (1H, s, protons at C_{13}), 7.20–7.70 (14H, m, protons at C_8–H, C_9–H, C_{10}–H, C_{11}–H, C_{12}–H, C_{15}–H, C_{16}–H, C_{18}–H, C_{19}–H, $C_{8'}$–H, $C_{9'}$–H, $C_{10'}$–H, $C_{11'}$–H, $C_{12'}$–H), 12.50 (1H, s, protons -OH), 13.80

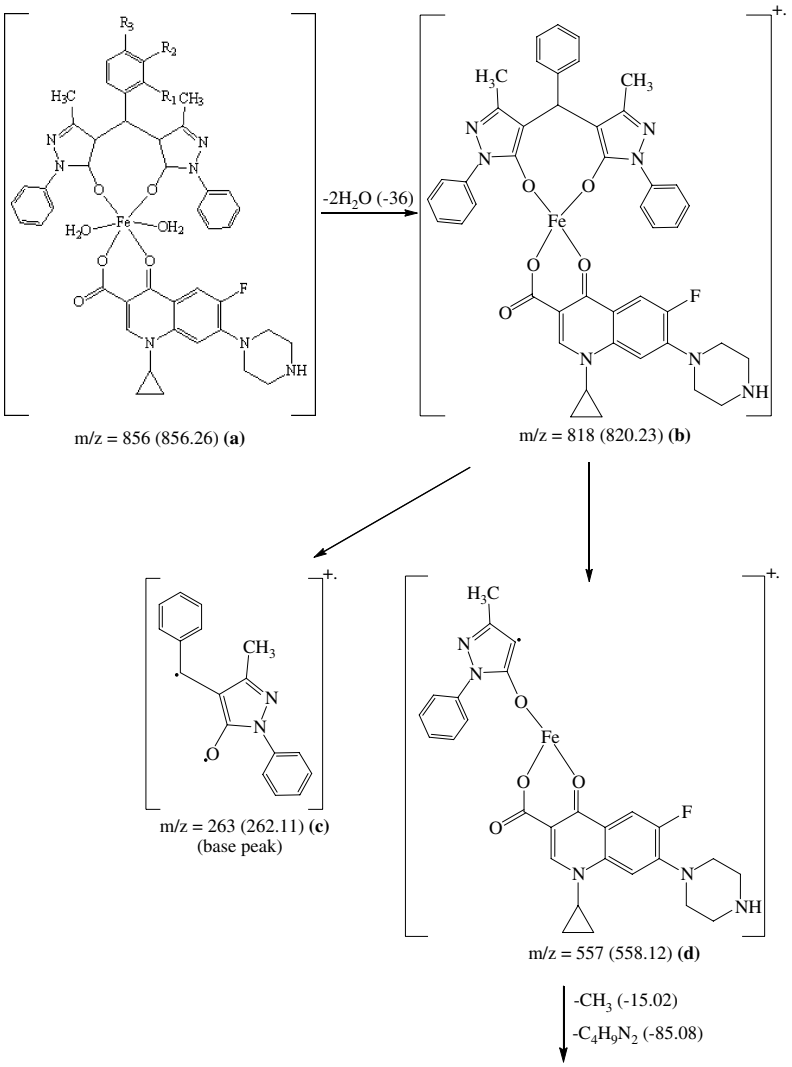

Scheme 2 The suggested fragmentation pattern of $[Fe(A^3)(L)(H_2O)_2]^{\bullet}2H_2O$.

(1H, s, protons H· · ·OH); ^{13}C-NMR: 12.02 (C_6, $C_{6'}$), 33.10 (C_{13}), 121.00 (C_4, $C_{4'}$), 126.00 (C_{10}, $C_{10'}$), 128.50 (C_8, C_{12}, $C_{8'}$, $C_{12'}$), 129.30 (C_9, C_{11}, C_{16}, C_{18}, $C_{9'}$, $C_{11'}$), 129.60 (C_{15}, C_{19}), 131.10 (C_{14}, C_{17}), 137.70 (C_7, $C_{7'}$), 141.60 (C_3, $C_{3'}$), 146.70 (C_5, $C_{5'}$); DEPT-135: 12.00 (C_6, $C_{6'}$), 33.10 (C_{13}), 121.00 (C_4, $C_{4'}$), 126.00 (C_{10}, $C_{10'}$), 128.50 (C_8, C_{12}, $C_{8'}$, $C_{12'}$), 129.30 (C_9, C_{11}, C_{16}, C_{18}, $C_{9'}$, $C_{11'}$), 129.60 (C_{15}, C_{19}).

4,4′-(Phenylmethylene)bis(3-methyl-1-phenyl-1H-pyrazol-5-ol) (H_2A^3)

H_2A^3 was synthesized by same method used for H_2A^1 by using benzaldehyde instead of 4-nitrobenzaldehyde. Yield, 80%; m.p. 171–173 °C. Found (%): C, 74.68, H, 5.37, N, 12.87. $C_{27}H_{24}N_4O_2$ (436.50) requires (%): C, 74.29, H, 5.53, N, 12.83. IR: 3410 (O–H), 1602 (C═O); ^{1}H-NMR: 2.20 (6H, s, protons at C_6, $C_{6'}$), 4.90 (1H, s, protons at C_{13}), 7.10–7.90 (14H, m, protons at C_8–H, C_9–H, C_{10}–H, C_{11}–H, C_{12}–H, C_{15}–H, C_{16}–H, C_{18}–H, C_{19}–H, $C_{8'}$–H, $C_{9'}$–H, $C_{10'}$–H, $C_{11'}$–H, $C_{12'}$–H), 12.40 (1H, s, protons -OH), 13.90 (1H, s, protons H· · ·OH); ^{13}C-NMR: 12.10 (C_6, $C_{6'}$), 33.60 (C_{13}), 121.00 (C_4, $C_{4'}$), 125.02 (C_8, C_{12}, $C_{8'}$, $C_{12'}$), 126.00 (C_{17}), 126.30 (C_{10}, $C_{10'}$), 127.60 (C_{16}, C_{18}), 128.60 (C_{15}, C_{19}), 129.30 (C_9, C_{11}, $C_{9'}$, $C_{11'}$), 137.80 (C_7, $C_{7'}$), 142.70 (C_{14}), 146.80 (C_3, $C_{3'}$), 149.80 (C_5, $C_{5'}$); DEPT-135: 12.10 (C_6, $C_{6'}$), 33.60 (C_{13}), 121.00 (C_4, $C_{4'}$), 126.00 (C_{17}), 126.30 (C_{10}, $C_{10'}$), 127.60 (C_{16}, C_{18}), 128.60 (C_{15}, C_{19}), 129.30 (C_8, C_{12}, $C_{8'}$, $C_{12'}$), 129.70 (C_9, C_{11},, $C_{9'}$, $C_{11'}$).

4,4′-[(4-Hydroxyphenyl)methylene]bis(3-methyl-1-phenyl-1H-pyrazol-5-ol) (H_2A^4)

H_2A^4 was synthesized by same method used for H_2A^1 by using 4-hydroxybenzaldehyde instead of 4-nitrobenzaldehyde. Yield, 82%; m.p. 152–153 °C. Found (%): C, 71.79, H, 5.35, N, 12.21. $C_{27}H_{24}N_4O_3$ (452.50) requires (%): C, 71.67, H, 5.34, N, 12.38. IR: 3402 (O–H), 1600 (C═O); ^{1}H-NMR: 2.30 (6H, s, protons at C_6, $C_{6'}$), 4.80 (1H, s, protons at C_{13}), 6.68–7.70 (14H, m, protons at C_8–H, C_9–H, C_{10}–H, C_{11}–H, C_{12}–H, C_{15}–H, C_{16}–H, C_{18}–H, C_{19}–H, $C_{8'}$–H, $C_{9'}$–H, $C_{10'}$–H, $C_{11'}$–H, $C_{12'}$–H), 12.30 (1H, s, protons -OH), 13.90 (1H, s, protons H· · ·OH); ^{13}C-NMR: 12.10 (C_6, $C_{6'}$), 32.90 (C_{13}), 115.30 (C_{16}, C_{18}), 120.90 (C_4, $C_{4'}$), 125.90 (C_8, C_{12}, $C_{8'}$, $C_{12'}$), 128.60 (C_{10}, $C_{10'}$), 129.30 (C_9, C_{11}, C_{15}, C_{19}, $C_{9'}$, $C_{11'}$), 132.70 (C_{14}), 137.90 (C_7, $C_{7'}$), 146.70 (C_3, $C_{3'}$), 156.00 (C_5, C_{17}, $C_{5'}$); DEPT-135: 12.10 (C_6, $C_{6'}$), 32.90 (C_{13}), 115.30 (C_{16}, C_{18}), 120.90 (C_4, $C_{4'}$), 125.90 (C_8, C_{12}, $C_{8'}$, $C_{12'}$), 128.60 (C_{10}, $C_{10'}$), 129.30 (C_9, C_{11}, C_{15}, C_{19}, $C_{9'}$, $C_{11'}$).

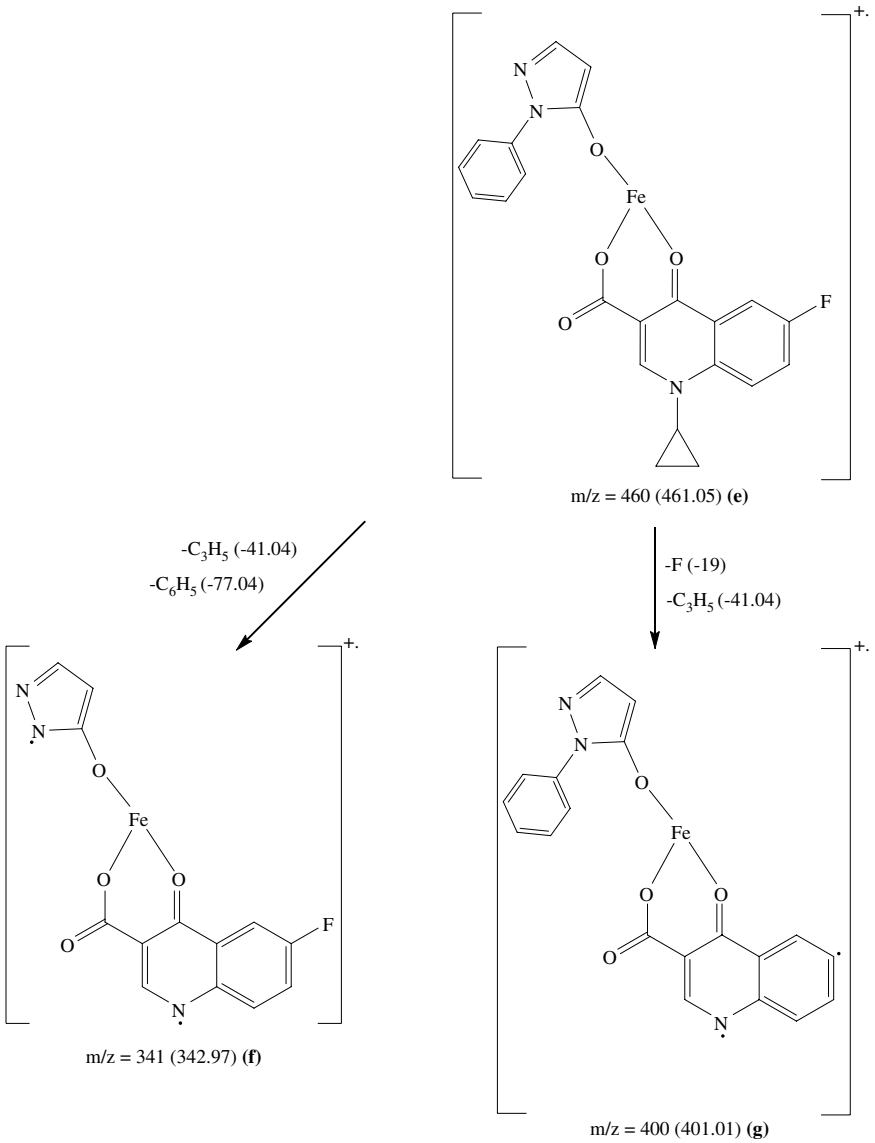

Scheme 2 (*Continued*).

4,4′-((4-methoxyphenyl)methylene)bis(3-methyl-1-phenyl-1H-pyrazol-5-ol) (H_2A^5)

H_2A^5 was synthesized by same method used for H_2A^1 by using 4-methoxybenzaldehyde instead of 4-nitrobenzaldehyde. Yield, 78%; m.p. 213–215 °C. Found (%): C, 72.12, H, 5.55, N, 11.88. $C_{28}H_{26}N_4O_3$ (466.52) requires (%): C, 72.08, H, 5.61, N, 12.00. IR: 3390 (O–H), 1602 (C═O); ^{1}H-NMR: 2.33 (6H, s, protons at C_6, $C_{6'}$), 3.70 (3H, s, protons -OCH_3), 4.90 (1H, s, protons C_{13}), 7.20–8.10 (14H, m, protons at C_8–H, C_9–H, C_{10}–H, C_{11}–H, C_{12}–H, C_{15}–H, C_{16}–H, C_{18}–H, C_{19}–H, $C_{8'}$–H, $C_{9'}$–H, $C_{10'}$–H, $C_{11'}$–H, $C_{12'}$–H), 12.40 (1H, s, protons -OH), 13.90 (1H, s, protons H···OH); ^{13}C-NMR: 12.00 (C_6, $C_{6'}$), 32.90 (C_{13}), 55.40 (carbon of -OCH_3 group), 114.00 (C_{16}, C_{18}), 120.90 (C_4, $C_{4'}$), 123.80 (C_8, C_{12}, $C_{8'}$, $C_{12'}$), 125.90 (C_{10}, $C_{10'}$), 128.60 (C_9, C_{11}, $C_{9'}$, $C_{11'}$), 129.30 (C_{14}, C_{15}, C_{19},), 134.50 (C_7, $C_{7'}$), 137.90 (C_3, $C_{3'}$), 146.70 (C_5, $C_{5'}$), 158.00 (C_{17}); DEPT-135: 12.00 (C_6, $C_{6'}$), 32.80 (C_{13}), 55.40 (carbon of -OCH_3 group), 113.90 (C_{16}, C_{18}), 120.90 (C_4, $C_{4'}$), 123.90 (C_8, C_{12}, $C_{8'}$, $C_{12'}$), 125.90 (C_{10}, $C_{10'}$), 128.60 (C_9, C_{11}, $C_{9'}$, $C_{11'}$), 129.30 (C_{14}, C_{15}, C_{19}).

4,4′-[(4-Hydroxy-3-methoxyphenyl)methylene]bis(3-methyl-1-phenyl-1H-pyrazol-5-ol) (H_2A^6)

H_2A^6 was synthesized by same method used for H_2A^1 by using 4-hydroxy-3-methoxybenzaldehyde instead of 4-nitrobenzaldehyde. Yield, 85%; m.p. 199–201 °C. Found (%): C, 69.78, H, 5.39, N, 11.69. $C_{28}H_{26}N_4O_4$ (482.52) requires (%): C, 69.70, H, 5.42, N, 11.61. IR: 3405 (O–H), 1610 (C═O); ^{1}H-NMR: 2.30 (6H, s, protons at C_6, $C_{6'}$), 3.60 (3H, s, protons -OCH_3), 4.80 (1H, s, proton at C_{13}), 6.90–7.82 (14H, m, protons at C_8–H, C_9–H, C_{10}–H, C_{11}–H, C_{12}–H, C_{15}–H, C_{16}–H, C_{18}–H, C_{19}–H, $C_{8'}$–H, $C_{9'}$–H, $C_{10'}$–H, $C_{11'}$–H, $C_{12'}$–H), 8.70 (1H, s, protons at C_{17}–OH), 12.30 (1H, s, protons -OH), 13.90 (1H, s, protons H···OH); ^{13}C-NMR: 12.10 (C_6, $C_{6'}$), 33.30 (C_{13}), 56.10 (carbon of -OCH_3 group), 112.50 (C_{15}), 115.60 (C_{18}), 120.10 (C_4, $C_{4'}$), 121.00 (C_8, C_{12}, C_{19}, $C_{8'}$, $C_{12'}$), 126.00 (C_{10}, $C_{10'}$), 129.30 (C_9, C_{11}, C_{14}, C_{19}, $C_{9'}$, $C_{11'}$), 133.70 (C_7, $C_{7'}$), 145.70 (C_3, $C_{3'}$), 148.30 (C_{17}), 155.60 (C_{16}), 157.76 (C_5, $C_{5'}$); DEPT-135: 12.00 (C_6, $C_{6'}$), 33.30 (C_{13}), 56.10 (carbon of -OCH_3 group), 112.40 (C_{15}), 115.60 (C_{18}), 120.10 (C_4, $C_{4'}$), 121.00 (C_8, C_{12}, C_{19}, $C_{8'}$, $C_{12'}$), 126.00 (C_{10}, $C_{10'}$), 129.04 (C_9, C_{11}, $C_{9'}$, $C_{11'}$).

Table 3. Minimum inhibitory concentrations (ppm) of the compounds against bacteria

Compounds	*Bacillus subtilis*	*Staphylococcus aureus*	*Escherichia coli*	*Serratia marcescens*
$Fe(NO_3)_3{\bullet}9H_2O$	750	600	600	600
Ciprofloxacin (HL)	0.4	0.6	0.5	0.6
H_2A^1	100	100	100	50
H_2A^2	200	100	100	200
H_2A^3	200	200	200	200
H_2A^4	100	100	100	100
H_2A^5	125	125	125	125
H_2A^6	125	100	100	100
H_2A^7	100	100	100	100
H_2A^8	125	125	125	167
H_2A^9	167	125	125	125
$[Fe(A^1)(L)(H_2O)_2]{\bullet}H_2O$	1.6	20	1.25	5
$[Fe(A^2)(L)(H_2O)_2]{\bullet}2H_2O$	5.0	20	5.0	20
$[Fe(A^3)(L)(H_2O)_2]{\bullet}2H_2O$	0.6	0.25	20	20
$[Fe(A^4)(L)(H_2O)_2]{\bullet}2H_2O$	1.0	10	10	–
$[Fe(A^5)(L)(H_2O)_2]{\bullet}2H_2O$	2.5	0.25	50	50
$[Fe(A^6)(L)(H_2O)_2]{\bullet}1.5H_2O$	2.5	0.25	20	20
$[Fe(A^7)(L)(H_2O)_2]{\bullet}1.5H_2O$	2.5	20	1.0	2.5
$[Fe(A^8)(L)(H_2O)_2]{\bullet}0.5H_2O$	1.6	5.0	0.25	5.0
$[Fe(A^9)(L)(H_2O)_2]{\bullet}H_2O$	1.0	1.25	1.0	10

4,4′-[(3-Nitrophenyl)methylene]bis(3-methyl-1-phenyl-1H-pyrazol-5-ol) (H_2A^7)

H_2A^7 was synthesized by same method used for H_2A^1 by using 3-nitrobenzaldehyde instead of 4-nitrobenzaldehyde. Yield, 87%; m.p. 230–232 °C. Found (%): C, 67.54, H, 4.83, N, 14.57. $C_{27}H_{23}N_5O_4$ (481.50) requires (%): C, 67.35, H, 4.81, N, 14.54. IR: 3398 (O–H), 1612 (C═O); ^{1}H-NMR: 2.20 (6H, s, protons at C_6, $C_{6'}$), 5.40 (1H, s, proton at C_{13}), 7.20–7.70 (14H, m, protons at C_8–H, C_9–H, C_{10}–H, C_{11}–H, C_{12}–H, C_{15}–H, C_{16}–H, C_{18}–H, C_{19}–H, $C_{8'}$–H, $C_{9'}$–H, $C_{10'}$–H, $C_{11'}$–H, $C_{12'}$–H), 12.60 (1H, s, protons -OH), 13.30 (1H, s, protons H···OH). ^{13}C-NMR: 11.90 (C_6, $C_{6'}$), 29.80 (C_{13}), 121.00 (C_4, $C_{4'}$), 124.50 (C_8, C_{12}, $C_{8'}$, $C_{12'}$), 126.10 (C_{10}, $C_{10'}$), 128.20 (C_{17}), 128.60 (C_{16}), 129.02 (C_9, C_{11}, $C_{9'}$, $C_{11'}$), 130.50 (C_{19}), 132.30 (C_{14}), 134.70 (C_{18}), 137.64 (C_7, $C_{7'}$), 146.40 (C_3, $C_{3'}$), 149.70 (C_{15}), 152.76 (C_5, $C_{5'}$). DEPT-135: 12.10 (C_6, $C_{6'}$), 29.90 (C_{13}), 116.70 (C_{18}), 121.00 (C_4, $C_{4'}$), 124.50 (C_8, C_{12}, $C_{8'}$, $C_{12'}$), 128.20 (C_{10}, $C_{10'}$), 129.40 (C_9, C_{11}, $C_{9'}$, $C_{11'}$), 130.50 (C_{19}), 132.30 (C_{15}).

4,4′-[(2-Nitrophenyl)methylene]bis(3-methyl-1-phenyl-1H-pyrazol-5-ol) (H_2A^8)

H_2A^8 was synthesized by same method used for H_2A^1 by using 2-nitrobenzaldehyde instead of 4-nitrobenzaldehyde. Yield, 84%; m.p. 148–150 °C. Found (%): C, 67.40, H, 4.82, N, 14.60. $C_{27}H_{23}N_5O_4$ (481.50) requires (%): C, 67.35, H, 4.81, N, 14.54. IR: 3402 (O–H), 1601 (C═O); ^{1}H-NMR: 2.34 (6H, s, protons at C_6, $C_{6'}$), 5.10 (1H, s, proton at C_{13}), 7.20–8.10 (14H, m, protons at C_8–H, C_9–H, C_{10}–H, C_{11}–H, C_{12}–H, C_{15}–H, C_{16}–H, C_{18}–H, C_{19}–H, $C_{8'}$–H, $C_{9'}$–H, $C_{10'}$–H, $C_{11'}$–H, $C_{12'}$–H), 12.60 (1H, s, protons -OH), 13.80 (1H, s, protons H···OH). ^{13}C-NMR: 12.00 (C_6, $C_{6'}$), 33.40 (C_{13}), 121.60 (C_4, $C_{4'}$), 121.10 (C_8, C_{12}, $C_{8'}$, $C_{12'}$), 126.20 (C_{10}, $C_{10'}$), 122.20(C_{17}), 129.40 (C_9, C_{11}, C_{15}, C_{19}, $C_{9'}$, $C_{11'}$), 130.1 (C_{18}), 134.8 (C_{19}), 136.10 (C_{14}), 137.60 (C_7, $C_{7'}$), 145.10 (C_3, $C_{3'}$), 146.55 (C_{17}), 148.20 (C_5, $C_{5'}$); DEPT-135: 12.00 (C_6, $C_{6'}$), 33.30 (C_{13}), 116.80 (C_{16}), 121.60 (C_4, $C_{4'}$), 121.10 (C_8, C_{12}, $C_{8'}$, $C_{12'}$), 122.20 (C_{17}), 126.20 (C_{10}, $C_{10'}$), 129.40 (C_9, C_{11}, C_{15}, $C_{9'}$, $C_{11'}$), 130.10 (C_{18}), 134.80 (C_{19}).

4,4′-(p-Tolylmethylene)bis(3-methyl-1-phenyl-1H-pyrazol-5-ol) (H_2A^9)

H_2A^9 was synthesized by same method used for H_2A^1 by using 4-methylbenzaldehyde instead of 4-nitrobenzaldehyde. Yield, 86%; m.p. 203–204 °C. Found (%): C, 72.77, H, 5.63, N, 12.18. $C_{28}H_{26}N_4O_2$ (462.54) requires (%): C, 72.70, H, 5.66, N, 12.11. IR: 3410 (O–H), 1599 (C═O); ^{1}H-NMR: 2.30 (6H, s, protons at C_6, $C_{6'}$), 2.20 (3H, s, protons -CH_3), 4.90 (1H, s, protons -CH), 7.00–7.70 (14H, m, protons at C_8–H, C_9–H, C_{10}–H, C_{11}–H, C_{12}–H, C_{15}–H, C_{16}–H, C_{18}–H, C_{19}–H, $C_{8'}$–H, $C_{9'}$–H, $C_{10'}$–H, $C_{11'}$–H, $C_{12'}$–H), 12.40 (1H, s, protons -OH), 13.90 (1H, s, protons H···OH). ^{13}C-NMR: 12.00 (C_6, $C_{6'}$), 21.0 (carbon of -CH_3 group), 33.20 (C_{13}), 120.90 (C_4, $C_{4'}$), 125.90 (C_8, C_{12}, $C_{8'}$, $C_{12'}$), 127.50 (C_{10}, $C_{10'}$), 129.10 (C_{15}, C_{16}, C_{18}, C_{19}), 129.30 (C_9, C_{11}, $C_{9'}$, $C_{11'}$), 135.20 (C_{14}, C_{17}, C_{19}), 137.80 (C_7, $C_{7'}$), (C_3, $C_{3'}$), 146.70 (C_5, $C_{5'}$). DEPT-135: 12.10 (C_6, $C_{6'}$), 21.0 (carbon of -CH_3 group), 33.20 (C_{13}), 120.90 (C_4, $C_{4'}$), 125.90 (C_8, C_{12}, $C_{8'}$, $C_{12'}$), 127.50 (C_{10}, $C_{10'}$), 129.10 (C_{15}, C_{16}, C_{18}, C_{19}), 129.30 (C_9, C_{11}, $C_{9'}$, C_{11}).

General Procedure for the Synthesis of Heterochelates

A methanolic solution (25 ml) of $Fe(NO_3)_3{\bullet}9H_2O$ (10 mmol) was added to hot methanolic solution (50 ml) of ligand (H_2A^n) (10 mmol), followed by addition of ciprofloxacin (HL) (10 mmol) in distilled water; the pH was adjusted to 6–7 with dilute NaOH solution in distilled water. The resulting solution was refluxed for 4 h at 70 °C and then heated over a steam bath to evaporate up to half of the volume. The reaction mixture was kept overnight at room temperature. A colored crystalline product was obtained. The obtained product was washed with water, methanol and finally with ether and dried over vacuum desiccators.

Minimum Inhibitory Concentration Value

The minimal inhibitory concentration (MIC) was ascertained using serial tube dilution technique[33] by variation of compound concentration. The antibacterial activity of the control, standard drug

Table 4. Electronic spectral data of free ligands (H_2A^n) and their heterochelates

Compounds	ILCT ($\pi \rightarrow \pi^*$) transition in cm^{-1}	d–d transitions in cm^{-1}
H_2A^1	32 500	–
H_2A^2	32 600	–
H_2A^3	32 600	–
H_2A^4	32 500	–
H_2A^5	32 650	–
H_2A^6	32 600	–
H_2A^7	32 500	–
H_2A^8	32 550	–
H_2A^9	32 550	–
$[Fe(A^1)(L)(H_2O)_2]^{\bullet}H_2O$	32 400	20 200
		18 500
$[Fe(A^2)(L)(H_2O)_2]^{\bullet}2H_2O$	32 450	20 000
		18 500
$[Fe(A^3)(L)(H_2O)_2]^{\bullet}2H_2O$	32 200	20 000
		18 450
$[Fe(A^4)(L)(H_2O)_2]^{\bullet}2H_2O$	32 500	20 000
		–
$[Fe(A^5)(L)(H_2O)_2]^{\bullet}2H_2O$	32 400	20 350
		–
$[Fe(A^6)(L)(H_2O)_2]^{\bullet}1.5H_2O$	32 500	20 000
		18 200
$[Fe(A^7)(L)(H_2O)_2]^{\bullet}1.5H_2O$	32 350	20 200
		–
$[Fe(A^8)(L)(H_2O)_2]^{\bullet}0.5H_2O$	32 200	20 050
		–
$[Fe(A^9)(L)(H_2O)_2]^{\bullet}H_2O$	32 400	20 200
		–

(ciprofloxacin), ligands (H_2A^n), metal salts and its heterochelates were screened for their anti-bacterial activity using different bacterial strains such as *Staphylococcus aureus, Bacillus subtilis, Escherichia coli* and *Serratia marcescens*. All the compounds were found to be more potent against bacterial strains with different MIC values.

Results and Discussion

The structural investigation of all the prepared ligands (H_2A^n) was done using elemental analyses, IR, ^{1}H- and ^{13}C-NMR and DEPT-135 spectroscopy. The heterochelates were prepared by reacting ferric nitrate with ciprofloxacin (HL) and variable ligands (H_2A^1–H_2A^9) in a 1 : 1 : 1 ratio. The analytical and physical data of the heterochelates are given in Table 1. The following chemical reaction describes the formation of the heterochelates:

$$Fe(NO_3)_3{}^{\bullet}9H_2O + H_2A^n + HL \longrightarrow [Fe(A^n)(L)(H_2O)_2]^{\bullet} mH_2O + (7-m)H_2O + 3HNO_3$$

where $n = 1$ and 9, $m = 1$; $n = 2$–5, $m = 2$; $n = 6$ and 7, $m = 1.5$; $n = 8$, $m = 0.5$.

All the heterochelates are insoluble in water, ethanol, methanol, chloroform, acetonitrile, CCl_4 and hexane, while soluble in DMF and DMSO, so it is difficult to grow single crystals for X-ray diffraction analysis.

IR Spectra

The important infrared spectral bands and their tentative assignments for the synthesized heterochelates were recorded as KBr disks and the data are presented in Table 2. All the ligands (H_2A^n) in the present investigation exhibit a broad band centered at 3390–3410 cm^{-1}. We assigned this peak to $\nu_{(O-H)}$ for the intramolecular hydrogen-bonded (H···O–H) form between two 5-OH groups, which was further confirmed by ^{1}H- and ^{13}C-NMR studies in solution state (discussed below). It also suggested that the ligands (H_2A^n) exist in enol form in both the states. The reaction of the enolic ligands with Fe^{3+} ion is revealed by the presence of a new band in the spectra of heterochelates at 1303–1316 cm^{-1} due to the $\nu_{(C-O)}$ (enolic).[34]

In the investigated heterochelates, the bands observed in the region 3418–3437, 1278–1295, 865–875 and 705–710 cm^{-1} are attributed to -OH stretching, bending, rocking and wagging vibrations, respectively, due to the presence of water molecules. The presence of rocking band indicates the coordination nature of the water molecule.[35]

Comparing the main IR frequencies of Fe(III) heterochelates with that of ciprofloxacin (HL) ligand (Table 2), the following results were found. Two very strong absorption peaks in the spectrum of the ligand were observed at 1707 and 1635 cm^{-1} due to $\nu_{(O-H)}$ of the carboxylic group and $\nu_{(C=O)}$ group, respectively. Absence of the former band in the spectra of the heterochelates suggests that this moiety participated in the bonding to the metal ion.[36] The later band corresponding to $\nu_{(C=O)}$ shifted to the lower frequency region (~1624 cm^{-1}) in the spectra of the heterochelates could be due to coordination through either the ketone group or the carboxylic group bonded to the metal ion. We confirm that the coordination was through the ketonic group of the HL ligand as the antisymmetric and symmetric modes of the carboxylate group were observed at 1618 and 1384 cm^{-1}, respectively. The $\nu_{as(COO^-)}$ and $\nu_{s(COO^-)}$ vibrational frequencies, together with the $\nu_{(COO^-)}$ values for the carboxylate group of the ciprofloxacin (HL) ligand and their heterochelates are listed in Table 2. The heterochelates produced a $\Delta\nu$ value of >200 cm^{-1}, suggesting unidentate carboxylate coordination to the central metal ions.[37–39] Accordingly ciprofloxacin (HL), in the isolated heterochelates appears to act as a uninegative bidentate ligand through the oxygen atom of the carbonyl group and enolic oxygen of the carboxylate group.

In the far-IR region, two new bands at 444–472 and 410–430 cm^{-1} in the heterochelates were assigned to $\nu_{(M-O)}$ pyrazolone and $\nu_{(M-O)}$ ketone of HL modes, respectively. All of these data confirm the fact that bis-pyrazolones (H_2A^n) behave as dinegative bidentate ligands forming a conjugated chelate ring with existing heterochelates in the enolized form.

^{1}H- and ^{13}C-NMR Spectra of the Ligands (H_2A^n)

Structural analysis of the ligands was carried out with the help of ^{1}H- and ^{13}C-NMR using DMSO-d_6 at room temperature. The data are presented in the Experimental section. In the case of ^{1}H-NMR spectra for the ligand, two broad singlets equivalent to one proton each were observed around δ 12.30–12.60 and 13.30–13.90 ppm corresponding to O–H and H···O–H groups, respectively. These signals disappeared when a D_2O exchange experiment was carried out. The later peak was observed in the strongly deshielded region because of hydrogen bonding (H···O–H) with the other oxygen atom of the 5-OH group of the remaining pyrazolone moiety. It shows the enolic nature of ligand and the broadness of these

Table 5. Thermo analytical data of the heterochelates

Heterochelates	TG range (°C)	DTGmax (°C)	DSCmax (°C)	Mass loss (%) obs. (calcd.)	Assignment
$[Fe(A^1)(L)(H_2O)_2]^{\bullet}H_2O$	50–110	–	–	1.90 (1.95)	Loss of one lattice water molecules
	110–190	160	134.12 (+)	3.85 (3.92)	Loss of two coordinated water molecules
	190–475	390	272.12 (−)	35.80 (35.93)	Loss of HL ligand
	475–800	–	–	49.68 (49.55)	Loss of remaining A^1 ligand leaving Fe_2O_3 residue
				91.23 (91.35)	
$[Fe(A^2)(L)(H_2O)_2]^{\bullet}2H_2O$	50–210	172	–	7.70 (7.77)	Loss of two lattice + two coordinated water molecules
	210–335	275	191.93, 291.52	35.37 (35.66)	Loss of HL ligand
	335–800	–	(−)	48.33 (48.03)	Loss of remaining A^2 ligand leaving Fe_2O_3 residue
			–	91.40 (91.46)	
$[Fe(A^3)(L)(H_2O)_2]^{\bullet}2H_2O$	50–115	–	104.37 (+)	3.96 (4.03)	Loss of two lattice water molecules
	115–190	160	–	3.92 (4.03)	Loss of two coordinated water molecules
	190–430	295	184.63, 269.11 (−)	37.18 (37.02)	Loss of HL ligand
	430–800	730	–	46.19 (46.00)	Loss of remaining A^3 ligand Leaving Fe_2O_3 residue
				91.25 (91.08)	
$[Fe(A^4)(L)(H_2O)_2]^{\bullet}2H_2O$	50–105	–	–	3.99 (3.96)	Loss of two lattice water molecules
	105–190	165	130.12 (+)	3.90 (3.96)	Loss of two coordinated water molecules
	190–425	290	182.43, 266.10 (−)	56.96	Loss of HL ligand + some part of A^4 ligand
	425–800	520	–	26.23	Loss of remaining part of A^4 ligand Leaving Fe_2O_3 residue
$[Fe(A^5)(L)(H_2O)_2]^{\bullet}2H_2O$	50–195	170	84.89 (+)	7.75 (7.80)	Loss of two lattice + two coordinated water molecules
	195–455	255	208.77 (−)	35.58 (35.81)	Loss of HL ligand
	455–600	480	–	47.89 (47.76)	Loss of remaining A^5 ligand leaving Fe_2O_3 residue
				91.22 (91.37)	
$[Fe(A^6)(L)(H_2O)_2]^{\bullet}1.5H_2O$	50–190	–	103.08 (+)	6.67 (6.77)	Loss of 1.5 lattice + two coordinated water molecules
	190–350	273	195.31 (−)	35.42 (35.54)	Loss of HL ligand
	350–500	–	353.70 (−)	49.29 (49.12)	Loss of remaining A^6 ligand leaving Fe_2O_3 residue
				91.38 (91.43)	
$[Fe(A^7)(L)(H_2O)_2]^{\bullet}1.5H_2O$	50–95	–	94.31 (+)	2.87 (2.90)	Loss of 1.5 lattice water molecules
	95–195	180	–	3.79 (3.87)	Loss of two coordinated water molecules
	195–455	333	203.47 (−)	58.65	Loss of HL ligand + some part of A^7 ligand
	455–700	530	–	26.15	Loss of remaining part of A^7 ligand Leaving Fe_2O_3 residue
$[Fe(A^8)(L)(H_2O)_2]^{\bullet}0.5H_2O$	50–220	200	134.69 (+)	4.88 (4.94)	Loss of 0.5 lattice + two coordinated water molecules
	220–465	410	193.73 (−)	36.15 (36.29)	Loss of HL ligand
	465–700	–	–	50.22 (50.04)	Loss of remaining A^8 ligand leaving Fe_2O_3 residue
				91.25 (91.27)	
$[Fe(A^9)(L)(H_2O)_2]^{\bullet}H_2O$	50–120	–	–	1.98 (2.02)	Loss of one lattice water molecules
	120–185	–	137.35 (+)	3.94 (4.04)	Loss of two coordinated water molecules
	185–495	285	188.22, 271.00 (−)	37.05 (37.18)	Loss of HL ligand
	495–800	–	–	49.33 (49.14)	Loss of remaining A^9 ligand leaving Fe_2O_3 residue
				92.30 (92.38)	

(+): Endothermic; (−): exothermic.

Table 6. Kinetic parameters of the heterochelates

Heterochelates	TG range (°C)	E_a (kJ mol^{-1})	n	A (s^{-1})	S^* (J K^{-1} mol^{-1})	H^* (kJ mol^{-1})	G^* (kJ mol^{-1})
$[Fe(A^1)(L)(H_2O)_2]^{\bullet}H_2O$	50–110	3.26	0.98	0.129	−102.34	.60	33.66
	110–190	7.77	0.98	0.358	−100.46	4.00	49.51
	190–475	22.23	1.00	12.23	−96.75	26.32	90.46
	475–800	31.83	0.99	28.05	−95.35	28.44	95.35
$[Fe(A^2)(L)(H_2O)_2]^{\bullet}2H_2O$	50–210	3.09	0.99	0.112	−102.57	0.408	33.53
	210–335	5.24	1.00	0.123	−101.88	1.478	47.63
	335–800	16.14	1.00	1.930	−98.61	11.468	66.98
$[Fe(A^3)(L)(H_2O)_2]^{\bullet}2H_2O$	50–115	3.45	0.99	0.144	−102.17	0.772	33.77
	115–190	5.82	1.00	0.160	−101.50	2.057	48.04
	190–430	11.52	1.00	4.002	−98.06	13.84	68.07
	430–800	18.43	0.98	6.023	−94.43	33.51	70.05
$[Fe(A^4)(L)(H_2O)_2]^{\bullet}2H_2O$	50–105	3.19	0.98	0.120	−102.45	0.508	33.60
	105–190	5.23	0.99	0.132	−101.81	1.549	46.65
	190–425	12.88	1.00	0.767	−99.42	8.205	64.18
	425–800	28.48	1.01	9.721	−95.63	18.48	65.51
$[Fe(A^5)(L)(H_2O)_2]^{\bullet}2H_2O$	50–195	3.34	1.00	0.078	−102.90	0.162	39.57
	195–455	9.65	1.00	0.733	−99.68	5.884	51.04
	455–600	14.00	0.99	0.398	−99.87	8.241	77.45
$[Fe(A^6)(L)(H_2O)_2]^{\bullet}1.5H_2O$	50–190	3.39	1.01	0.074	−102.94	0.128	40.58
	190–350	13.68	1.00	2.133	−98.65	09.67	57.32
	350–500	49.26	1.00	17.52	−95.00	44.00	104.14
$[Fe(A^7)(L)(H_2O)_2]^{\bullet}1.5H_2O$	50–95	3.36	1.01	0.072	−102.99	0.083	40.55
	95–195	7.51	0.98	0.215	−100.96	3.334	54.12
	195–455	15.98	1.00	0.483	−99.62	9.802	72.32
	455–700	22.23	0.99	13.554	−93.45	11.13	82.82
$[Fe(A^8)(L)(H_2O)_2]^{\bullet}0.5H_2O$	50–220	3.30	1.00	0.065	−103.13	−0.04	41.51
	220–465	8.42	0.98	0.169	−101.08	3.57	62.51
	465–700	20.76	1.00	3.543	−98.06	15.58	76.68
$[Fe(A^9)(L)(H_2O)_2]^{\bullet}H_2O$	50–120	3.32	1.00	0.077	−102.92	0.140	39.56
	120–185	10.63	0.99	0.674	−99.67	6.499	56.13
	185–495	22.25	1.00	34.43	−95.55	26.13	73.22
	495–800	31.10	1.01	54.55	−96.46	33.42	83.81

two singlets due to fast exchange interaction of proton via keto-enol tautomerism. It may be noted that the integration of these signals perfectly matches with one proton each. We did not do any temperature-dependent experiments. Comparing with the solid-state study, we prefer to assign these signals to O–H and H···O–H; however, the provided solid-state structural evidence has not been considered.

In the case of ^{1}H-NMR spectra of the ligand, peaks observed at ~6.68–8.10 ppm were assigned to the aromatic protons. The two singlet peaks at ~5.10 and ~2.30 ppm were assigned to aliphatic proton (C_{13}–H) and six protons of two -CH_3 groups of bis-pyrazolones, respectively. In ^{13}C-NMR spectra peaks observed at 124–138 ppm were assigned to aromatic carbons. Peak observed at ~157 was assigned to C–O of C_5, $C_{5'}$ carbons. Aliphatic carbon (C_{13}) was observed at ~33 ppm.

FAB Mass Spectra

The recorded FAB mass spectrum (Fig. 1) and the molecular ion peak for the heterochelate $[Fe(A^3)(L)(H_2O)_2]^{\bullet}2H_2O$ were used to confirm the molecular formulae. The proposed fragmentation pattern is shown in Scheme 2. The first peak at *m/z* 856 represents the molecular ion peak of the heterochelate (without water of crystallization). Scheme 2 demonstrates the possible degradation pathway for the investigated heterochelate. The primary fragmentation of the heterochelate takes place due to the loss of two coordinated H_2O molecules from the species (a) to give species (b) with peak at *m/z* 818. The species (b) further degrades to give species (d) with loss of species (c). The sharp peak (base peak) observed at *m/z* 263 represents the stable species (c) with 99.5% abundance. Species (d) further degrades with the loss of -CH_3 and -$C_4H_9N_2$ moieties forming species (e) with a peak at *m/z* 460. Species (e) has two possibilities for degradation, either degrading with the loss of -C_6H_5 and -C_3H_5 moieties to give species (f) (*m/z* 341) or degrading with the loss of -C_3H_5 and -F moieties to give species (g) with a peak at *m/z* 400. The measured molecular weights for all the suggested degradation steps were consistent with expected values.

Antibacterial Screening

The antibacterial activity of the control, standard drug (ciprofloxacin), metal salts, ligands (H_2A^n) and their heterochelates were screened against different bacterial strains as stated above.

Staphylococcus aureus is the preliminary screening test organism of choice for several reasons. It is a systemic pathogen and seems to develop antibiotic resistance more readily than any other bacteria, and laboratory animals can be readily infected with it. The inhibition of growth of these Gram-positive organisms produced by various concentrations of the test compounds were compared under identical conditions with the inhibition of growth of the same organism by ciprofloxacin, which is a standard antibiotic and resists the growth of organism. Similarly, the inhibitions of the Gram-negative organism growth produced by the test compounds were compared with those for the same concentrations of ciprofloxacin, which is a broad-spectrum antibiotic.

A standard volume (5 ml) of Luria broth medium (2%) to support the growth of the test organism was added to several labeled sterile stopper identical assay tubes. A solution of each test compound was prepared in DMSO and a series of dilutions was prepared. Concentrations tested were 0.25–20 ppm of the ligands and their heterochelates under investigation, a broad-spectrum antibiotic, the respective metal salt (20–800 ppm) dissolved in DMSO and a blank (DMSO). A control tube containing no test compound was also included. A 0.1 ml aliquot of the test organism from the overnight grown test cultures was added. All these operations were carefully performed under aseptic conditions. Assay tubes were incubated at 30 °C for 24 h. The resultant turbidities were measured using a Systronics spectrophotometer model no. 106. The minimum inhibitory concentration (MIC) of a test compound is the lowest concentration showing no visible turbidity. However, the final concentration of bacterial growth inhibition produced by a certain concentration of the test compound was calculated using the following relationship:

$$\%\text{inhibition} = \frac{T_c - T_t}{T_c} \times 100$$

where T_c is the turbidity of the control and T_t is the turbidity of the specific treatment or the test compound.

The heterochelates exhibited strong activities against two Gram-negative (*Escherichia coli, Serratia marcescens*) and two Gram-positive (*Staphylococcus aureus, Bacillus subtilis*) microorganisms. The antimicrobial activity data of the compounds are summarized in Table 3. Comparative analysis showed higher antibacterial activity of the heterochelates than free ligands and metal salt. Some of the heterochelates exhibited moderate activities as compared with the standard drug ciprofloxacin. It was also observed that some of the heterochelates were more potent bactericides than the ligands. This enhancement in antibacterial activity is rationalized on the basis of Overtone's concept, Tweedy's chelation theory and the partial sharing of the positive charge of metal ions with donor groups.[40–44] This may support the argument that some type of bimolecular binding to the metal ions or intercalation or electrostatic interaction causes the inhibition of biological synthesis and prevents the organisms from reproducing. The results of our studies (Table 3) indicate that compounds **3, 5** and **6** have good activity against *Staphylococcus aureus*, while **8** has good activity against *Escherichia coli*, displaying high affinities towards most of the receptors. The strong antimicrobial activities of these compounds against tested organisms suggest further investigation on these compounds.

Electronic Spectra and Magnetic Moments

The information regarding geometry of the heterochelates was obtained from their electronic spectral data and magnetic moment

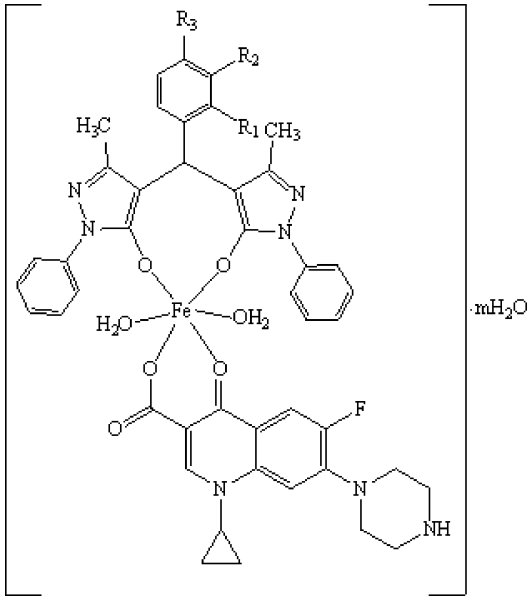

Heterochelates	R_1	R_2	R_3	mH_2O
1	-H	-H	$-NO_2$	$1H_2O$
2	-H	-H	-Cl	$2H_2O$
3	-H	-H	-H	$2H_2O$
4	-H	-H	-OH	$2H_2O$
5	-H	-H	$-OCH_3$	$2H_2O$
6	-H	$-OCH_3$	-OH	$1.5H_2O$
7	-H	$-NO_2$	-H	$1.5H_2O$
8	$-NO_2$	-H	-H	$0.5H_2O$
9	-H	-H	$-CH_3$	$1H_2O$

Figure 5. The proposed structure of heterochelates.

values. The electronic spectral data of the free ligands (H_2A^n) and their heterochelates are presented in Table 4. The diffused reflectance spectra of free ligands showed an intense band at 32 600 cm^{-1}. The high intensity of this band may be due to $\pi \rightarrow \pi^*$ intraligand charge transfer transition (ILCT). The reflectance spectra of heterochelates $[Fe(A^n)(L)(H_2O)_2]^{\bullet}mH_2O$ exhibited two additional bands at about ~20 000 and ~18 000 cm^{-1}, which were assigned to d–d transitions. In the case of compounds **4, 5, 7, 8** and **9**, the second band was not observed (Table 4), which is due to the greater absorption in the ultraviolet portion of the spectrum. From the electronic spectra, an octahedral geometry around the central metal ion is suggested.[45–47] This is further supported by the magnetic measurement data of Fe(III) heterochelates which falls in the range 5.90–6.01 B.M.

Thermal Studies

Each decomposition process follows the trend

$$\text{Solid-1} \xrightarrow{\text{heat}} \text{Solid-2} + \text{Gas}$$

This process comprises several stages. The method reported by Freeman and Carroll[48] has been adopted. Plots of $[\Delta\log(dw/dt)/\Delta\log wr]$ vs $[\Delta(1/T)/\Delta\log wr]$ were linear for all of

the decomposition steps. The energy of activation E_a was calculated from the slopes of these plots for a particular stage and the order of reactions (n) were determined from the intercept, showing first-order reaction over the entire range of decomposition for all the heterochelates. A typical plot for the thermal degradation of $[Fe(A^5)(L)(H_2O)_2]^{\bullet}2H_2O$ is shown in Fig. 2.

The Thermal Behavior of the Prepared Heterochelates

Thermal data and kinetic parameters of the heterochelates are given in Tables 5 and 6, respectively. The typical TG/DTG and DSC curves of the heterochelate $[Fe(A^5)(L)(H_2O)_2]^{\bullet}2H_2O$ are represented in Figs 3 and 4, respectively. The thermal fragmentation scheme for the heterochelates is shown below:

$$[Fe(A^n)(L)(H_2O)_2]\cdot mH_2O \xrightarrow[\text{removal of crystalline water molecules}]{50\text{–}120^\circ C} [Fe(A^n)(L)(H_2O)_2] + mH_2O$$

(Where $n = 1\&9$, $m = 1$; $n = 3\&4$, $m = 2$; $n = 7$, $m = 1.5$)

$$[Fe(A^n)(L)(H_2O)_2] \xrightarrow[\text{removal of coordinated water molecules}]{120\text{–}195^\circ C} [Fe(A^n)(L)] + 2H_2O$$

$$[Fe(A^n)(L)] \xrightarrow[\text{removal of HL ligand}]{195\text{–}495^\circ C} [Fe(A^n)]$$

$$[Fe(A^n)] \xrightarrow[\text{removal of } H_2A^n \text{ ligand}]{495\text{–}800^\circ C} Fe_2O_3$$

whereas for compounds **2, 5, 6** and **8** the thermal fragmentation scheme is shown below:

$$[Fe(A^n)(L)(H_2O)_2]\cdot mH_2O \xrightarrow[\text{removal of crystalline + coordinated water molecules}]{50\text{–}220^\circ C} [Fe(A^n)(L)] + 2H_2O + mH_2O$$

(Where $n = 2\&5$, $m = 2$; n = 6, $m = 1.5$; $n = 8$, $m = 0.5$)

$$[Fe(A^n)(L)] \xrightarrow[\text{removal of HL ligand}]{220\text{–}465^\circ C} [Fe(A^n)]$$

$$[Fe(A^n)] \xrightarrow[\text{removal of } H_2A^n \text{ ligand}]{465\text{–}800^\circ C} Fe_2O_3$$

The anhydrous heterochelates show great thermal stability up to 190 °C, and in the third subsequent stage for heterochelates, the decomposition and combustion of ligand (HL) occurs. In the fourth subsequent stage for heterochelates, the decomposition and combustion of ligand (H_2A^n) occurs. The removal of ligand (H_2A^n) undergoes decomposition, forming Fe_2O_3 as the final residue.

The thermodynamic activation parameters of the decomposition process of dehydrated heterochelates such as activation entropy (S^*), pre-exponential factor (A), activation enthalpy (H^*) and free energy of activation (G^*) were calculated using reported equations.[49] According to the kinetic data obtained from DTG curves, all the heterochelates have negative entropy, which indicates that the studied heterochelates have more ordered systems.[50] The energy of activation (E_a) is helpful in assigning the strength of the bonding of ligand moieties with the metal ion. The relatively high E_a value (Table 6) indicates that both the ligands are strongly bonded to the metal ion.[37] The thermal stabilities of the heterochelates **1, 3, 4, 7** and **9** in the solid state follow the general trend found by Irving and Williams[51] for the stabilities of complexes in solution. The heterochelates **2, 5, 6** and **8** deviate from this general behavior. Since the Irving-Williams series reflects electrostatic effects, this observation indicates that the water–metal interaction in these heterochelates is almost of ion-dipole type. A similar relationship was observed in the case of the double ammonium sulfate hexahydrate salts of the first raw transition metals.[52] From the above discussion an octahedral structure of the heterochelates can tentatively be assumed, as shown in Fig. 5.

Conclusions

The results obtained in this study allow the following conclusions:

1. The design and synthesis of new bis-pyrazolone ligands (H_2A^n) have successfully been demonstrated. FT-IR, ^{1}H-NMR, ^{13}C-NMR and DEPT-135 spectral studies reveal that ligands exist in the tautomeric enol form both in solid and solution states with intramolecular hydrogen bonding. We have synthesized a series of some novel drug based Fe(III) heterochelates with bis-pyrazolone derivatives and quinolone-based drug (HL) and characterized their properties.
2. All the synthesized compounds were screened for their bioassay. The heterochelates exhibited strong activities against two Gram-negative (*Escherichia coli, Serratia marcescens*) and two Gram-positive (*Staphylococcus aureus, Bacillus subtilis*) microorganisms. In comparison with both the ligands and metal salt, the Fe(III) heterochelates were more active against one or more bacterial strains, thus introducing a novel class of metal-based bactericidal agents.
3. The information regarding geometry of the heterochelates was obtained from their electronic and magnetic moment values. Magnetic moment values indicate that Fe(III) heterochelates are high-spin, lacking exchange interactions. The studies reveal that an octahedral geometry can be assigned to heterochelates.

Acknowledgments

We express our gratitude to Department of Chemistry, Bhavnagar University, Bhavnagar and Sardar Patel University, Vallabh Vidyanagar, India for providing laboratory facilities. We expressed our gratitude to Miss B. Kavita, research student, Department of Bio Sciences, Sardar Patel University for her valuable support. Analytical facilities provided by the SAIF, Central Drug Research Institute, Lucknow, India and the Sophisticated Instrumentation Centre for Applied Research and Testing (SICART), Vallabh Vidyanagar, Gujarat, India is gratefully acknowledged.

References

[1] E. C. Theil, *Iron Biomineralization* (Ed.: R. B. Frankel). Plenum Press: London, **1990**.
[2] P. B. Pansuriya, M. N. Patel, *Appl. Organomet. Chem.* **2007**, *21*, 926.
[3] M. Benigno, V. Marya, R. Inmaculada, *J. Inorg. Biochem.* **2001**, *84*, 163.
[4] A. M. Jamil, *Acta Chim. Slov.* **2002**, *49*, 457.
[5] K. S. Dilip, P. Subhash, *Trans. Met. Chem.* **2003**, *28*, 579.
[6] R. A. Juan, T. Caredmy, *Trans. Met. Chem.* **2001**, *26*, 228.
[7] I. Turel, *Coord. Chem. Rev.* **2002**, *232*, 27.
[8] N. Raman, A. Kulandaisamy, A. Shunmugasundaram, K. Jeyasubramanian, *Trans. Met. Chem.* **2001**, *26*, 131.

[9] B. A. Uzoukwu, P. U. Adiukwu, S. S. Al-Juaid, P. B. Hitchcock, J. D. Smith, *Inorg. Chim. Acta* **1996**, *250*, 173.
[10] Z. Y. Yang, R. D. Yang, F. S. Li, K. B. Yu, *Polyhedron* **2000**, *19*, 2599.
[11] W. F. Yang, S. G. Yuan, Y. B. Xu, Y. H. Xiao, K. M. Fang, *J. Radioanal. Nucl. Chem.* **2003**, *256*, 149.
[12] P. Chiba, W. Holzer, M. Landau, G. Bechmann, K. Lorenz, B. Plagens, M. Hitzler, E. Richter, G. Ecker, *J. Med. Chem.* **1998**, *41*, 4001.
[13] A. K. El-Sawaf, D. X. West, *Trans. Met. Chem.* **1998**, *23*, 417.
[14] N. Kalarani, S. Sangeetha, P. Kamalakannan, D. Venkappayya, *Russ. J. Coord. Chem.* **2003**, *29*, 845.
[15] T. Yoshikuni, *J. Mol. Catal. A: Chem.* **1999**, *148*, 285.
[16] F. Marchetti, C. Pettinari, R. Pettinari, A. Cingolani, D. Leonesi, A. Lorenzotti, *Polyhedron* **1999**, *18*, 3041.
[17] F. Marchetti, C. Pettinari, R. Pettinari, *Coord. Chem. Rev.* **2005**, *249*, 2909.
[18] J. S. Casas, M. S. García-Tasende, A. Sánchez, J. Sordo, Á. Touceda, *Coord. Chem. Rev.* **2007**, *251*, 1561.
[19] C. Pettinari, F. Marchetti, A. Drozdov, V. Vertlib, S. I. Troyanov, *Inorg. Chem. Commun.* **2001**, *4*, 290.
[20] C. Pettinari, F. Marchetti, R. Pettinari, A. Cingolani, A. Drozdov, S. I. Troyanov, *J. Chem. Soc. Dalton Trans.* **2002**, 188.
[21] S. N. Semenov, A. Yu. Rogachev, S. V. Eliseeva, C. Pettinari, F. Marchetti, A. A. Drozdov, S. I. Troyanov, *Chem. Commun.* **2008**, 1992.
[22] D. W. Johnson, J. Xu, R. W. Saalfrank, K. N. Raymond, *Angew. Chem. Int. Ed.* **1999**, *38*, 2882.
[23] J. Xu, K. N. Raymond, *Angew. Chem. Int. Ed.* **2000**, *39*, 2745.
[24] C. Pettinari, F. Marchetti, R. Pettinari, D. Martini, A. Drozdov, S. I. Troyanov, *J. Chem. Soc. Dalton Trans.* **2001**, 1790.
[25] L. Yang, R. Yang, *Polyhedron* **1995**, *14*, 507.
[26] X. Li, R. Yang, *Polyhedron* **1992**, *11*, 1545.
[27] L. Yang, R. Yang, *Acta Chim. Sinica* **1989**, *47*, 911.
[28] C. K. Modi, *Spectrochim. Acta Part A* **2009**, *71*, 1741.
[29] C. K. Modi, I. A. Patel, B. T. Thaker, *J. Coord. Chem.* **2008**, *61*(19), 3110.
[30] C. K. Modi, B. T. Thaker, *J. Therm. Anal. Cal.* **2008**, *94*(2), 567.
[31] A. I. Vogel, *Textbook of Practical Organic Chemistry*, 5th edn. Longman: London, **1989**.
[32] A. I. Vogel, *Textbook of Quantitative Inorganic Analysis*, 4th edn. ELBS and Longman: London, **1978**.
[33] M. J. Pelczar, R. D. Reid, E. C. S. Chan, *Microbiology*, 4th edn. Tata McGraw-Hill: New Delhi, **1979**.
[34] L. Liu, D. Jia, Y. Ji, *Synth. React. Inorg. Met.-Org. Chem.* **2002**, *32*, 739.
[35] N. Nakamoto, *Infrared Spectra and Raman Spectra of Inorganic and Coordination compounds*, John Wiley & Sons: New York, **1978**.
[36] L. Bellamy, *The Infrared Spectra of Complex Molecules*, 3rd edn. Chapman and Hall: London, **1975**.
[37] C. K. Modi, M. N. Patel, *J. Therm. Anal. Cal.* **2008**, *94*(1), 247.
[38] B. S. Creaven, D. A. Egan, K. Kavanagh, M. McCann, A. Noble, B. Thati, M. Walsh, *Inorg. Chim. Acta* **2006**, *359*, 3976.
[39] M. S. Masoud, M. F. Amira, A. M. Ramadana, G. M. El-Ashry, *Spectrochim. Acta Part A* **2008**, *69*, 230.
[40] Z. H. Chohan, *Appl. Organomet. Chem.* **2002**, *16*, 17.
[41] N. Dharmaraj, P. Viswanathamurthi, K. Natarajan, *Trans. Met. Chem.* **2001**, *26*, 105.
[42] Z. H. Chohan, K. M. Khan, C. T. Supuran, *Appl. Organomet. Chem.* **2004**, *18*, 305.
[43] P. K. Panchal, P. B. Pansuriya, M. N. Patel. *J. Enz. Inhib. Med. Chem.* **2006**, *21*(2), 203.
[44] F. Caruso, M. Rossi, J. Tanski, R. Sartori, R. Sariego, S. Moya, S. Diez, E. Navarrete, A. Cingolani, F. Marchetti, C. Pettinari, *J. Med. Chem.* **2000**, *43*, 3665.
[45] D. Danuta, B. J. Lucjan, D. Marek, *Polyhedron* **2005**, *24*, 407.
[46] F. A. Cotton, G. Wilkinson, The elements of first transition series, in *Avanced Inorganic Chemistry*, 3rd edn, Wiley: Chichester, **1992**.
[47] A. B. P. Lever, Electronic spectra of d^n ions, in *Inorganic Electronic Spectroscopy*, 2nd edn. Elsevier: Amsterdam, **1984**.
[48] E. S. Freeman, B. Carroll, *J. Phys. Chem.* **1958**, *62*, 394.
[49] C. K. Modi, S. H. Patel, M. N. Patel, *J. Therm. Anal. Cal.* **2007**, *87*, 441.
[50] M. E. El-Zaria, *Spectrochim. Acta Part A* **2008**, *69*, 216.
[51] H. Irving, R. J. P. Williams, *J. Chem. Soc.* **1953**, 3192.
[52] V. T. Yilmaz, H. Içbudak, H. Ölmez, *Thermochim. Acta* **1994**, *244*, 85.

